



# Characterization of High Power SiC Modules for More Electrical Aircrafts

Alaa Hilal, Bernardo Cougo, Thierry Meynard

## ► To cite this version:

Alaa Hilal, Bernardo Cougo, Thierry Meynard. Characterization of High Power SiC Modules for More Electrical Aircrafts. IECON 2016 (42nd Annual Conference of IEEE Industrial Electronics Society), 2016, Firenze, Italy. pp. 1087-1092. hal-01660829

**HAL Id: hal-01660829**

**<https://hal.science/hal-01660829>**

Submitted on 11 Dec 2017

**HAL** is a multi-disciplinary open access archive for the deposit and dissemination of scientific research documents, whether they are published or not. The documents may come from teaching and research institutions in France or abroad, or from public or private research centers.

L'archive ouverte pluridisciplinaire **HAL**, est destinée au dépôt et à la diffusion de documents scientifiques de niveau recherche, publiés ou non, émanant des établissements d'enseignement et de recherche français ou étrangers, des laboratoires publics ou privés.



## Open Archive TOULOUSE Archive Ouverte (OATAO)

OATAO is an open access repository that collects the work of Toulouse researchers and makes it freely available over the web where possible.

This is an author-deposited version published in : <http://oatao.univ-toulouse.fr/>  
Eprints ID : 18231

**To link to this article** : DOI: 10.1109/IECON.2016.7794111  
URL : <http://dx.doi.org/10.1109/IECON.2016.7794111>

**To cite this version** : Hilal, Alaa and Cougo, Bernardo and Meynard, Thierry *Characterization of High Power SiC Modules for More Electrical Aircrafts*. (2016) In: IECON 2016 (42nd Annual Conference of IEEE Industrial Electronics Society), 2016 - 2016 (Firenze, Italy).

Any correspondence concerning this service should be sent to the repository administrator: [staff-oatao@listes-diff.inp-toulouse.fr](mailto:staff-oatao@listes-diff.inp-toulouse.fr)

# Characterization of High Power SiC Modules for More Electrical Aircrafts

A. Hilal, B. Cougo  
More Electrical Aircraft Department  
IRT Saint-Exupery  
Toulouse, France  
alaa.hilal@irt-saintexupery.com

T. Meynard  
CNRS UMR5213 - LAPLACE Laboratory  
Institut National Polytechnique de Toulouse  
University of Toulouse, France  
thierry.meynard@laplace.univ-tlse.fr

**Abstract**—One of the main challenges associated to the More Electric Aircraft is to significantly increase power density of electrical power systems, such as electromechanical chains applied to actuation systems, without compromising on reliability. Nowadays, the best way of considerably increasing power density of power converters is by the use of disruptive technology such as Wide Bandgap (WBG) semiconductors.

This paper explains the advantages of using WBG semiconductors made of Silicon Carbide (SiC) in power converters used in an electromechanical chain when compared to classical silicon-based technology.

Characterization of a specific SiC power module is described in details. A non-intrusive method for measuring switching energy is explained and applied to this module in order to obtain turn-on and turn-off energies for different circuit and driver parameters. These results are used in a numerical routine which calculates losses in a three-phase inverter. These losses are compared to the ones calculated with the datasheet of this SiC module as well as with a “best-in-class” silicon-based IGBT adapted to the power level of this converter. Results show the superiority of SiC MOSFETs when compared to IGBTs as well as the highest performance which can be achieved with this component based on the characterization performed this paper.

**Keywords**—Power semiconductor devices, switching losses, measurements methods, More Electrical Aircraft (MEA), Silicon Carbide (SiC).

## I. INTRODUCTION

THE More Electric Aircraft (MEA) concept relies on replacing conventional non-electrical aircraft systems such as pneumatic, hydraulic, and mechanical systems with electrical ones [1]. The motivations behind this concept are similar to those for electrical vehicles including emissions reduction and decreasing fuel consumption [2]. Traditional aircrafts have different drawbacks compared to MEA, including the sacrifice of total engine efficiency in the process of harvesting a particular energy, as within hydraulic and pneumatic systems. In addition, non-electrical systems are less reliable and require more maintenance. The goal for future aircrafts is to replace most of the nonelectric systems, such as environmental controls and engine start, with new electrical systems to improve efficiency, CO<sub>2</sub> emissions, reliability, and maintenance costs.

One of the enabling technologies for MEA concept is the development of high power density power converters based on Wide BandGap (WBG) Semiconductors [3]. This WBG technology opened the door for more efficient systems in any aircraft power conversion application in the near future. In fact, Silicon Carbide (SiC) semiconductors are promising candidates to replace the Si semiconductors in this aspect [4]. The efficiency of SiC converters are significantly better than their Si counterparts due to the inherently lower conduction and switching losses of SiC MOSFETs compared to Si IGBTs [5]. Additionally, SiC components allow higher switching frequencies, which generally reduce the converter’s passive components volume, consequently increasing the converter’s power density. Moreover, SiC semiconductors may operate at higher junction temperature when compared to Si semiconductors, with the consequent reduction of the cooling system [6].

The goal of this paper is to show the characterization process for precise measurement of switching losses in order to find the best usage of such components in three-phase inverters concerning loss reduction.

Characterization not only regards energy loss during switching but also switching waveforms. These waveforms are specifically important when used to calculate overvoltage and voltage derivatives ( $dv/dt$ ) during commutation. This information is precious for precisely calculating filters so the converter can cope with EMI standards and to reduce Partial Discharge issues which may appear on cables and machines connected to the power converter. EMI and partial discharge issues will not be addressed in this paper.

Section II introduces the converter to be used as reference and also the SiC MOSFET power module to be characterized. Section III shows the characterization method in order to measure switching losses in WBG components. Section IV shows the experimental results of the switching loss characterization and the comments about it. Having these results, a comparison between IGBT and SiC MOSFET can be made concerning losses in transistors used in the reference power converter.

## II. SiC-MODULES FOR MEA POWER CONVERTERS

The shift of the aircraft industry towards MEA has given rise to many challenges in terms of electric power conversion technologies. Indeed, the high electric energy demand in the civilian aircrafts such as Airbus-A380 and Boeing-787 (up to four times the electrical energy in traditional aircrafts), forces the development of power converters with higher efficiency and power density.

However, in order to increase the power density of the whole electrical system, different systems concepts are proposed. One of these concepts is the Integrated Modular Power Electronics Cabinet (IMPEC), described in [7]. It consists of several power converters having the same characteristics which can be switched to supply several different loads inside an aircraft. Mutualization of these modular power converters can reduce volume, weight and cost of electrical power systems in modern aircrafts.

One of the ideas [8] is to produce standard modular power converters having the following characteristics:

- Topology: Three-phase inverter
- Power: 45kVA (nominal)
- DC bus voltage: 540V (nominal), 900V (maximum during transient).
- Output current: from 0 to 80A, per phase.

Generally, higher efficiency can be achieved by reducing the converter total losses, and higher power density can be achieved by increasing the switching frequency of the converter so to reduce the size of passive components. Both goals are achieved by using WBG components due to their high switching-frequency low-losses characteristics. For the characteristics of the converter described here above, SiC MOSFET having breakdown voltage of 1200V is a much better choice than Si-based IGBTs, as shown below as well as it will be shown in Section IV.

In [9] a 10kW hard-switching interleaved Boost DC/DC converter is developed to compare the performance of a 1200V/20A SiC MOSFET (C2M0080120D) with a Silicon high speed 1200V/40A IGBT (IGW40N120H3). Authors have shown that the key benefits for SiC MOSFET are the switching losses. Using a SiC at 100kHz instead of an IGBT at 20kHz reduced total switching losses from 20.5W to 13.8W. In fact, experimental results in [9] show that the Si IGBT turn-on energy is about twice and the turn-off energy is about ten times those of the SiC MOSFET due to IGBT current tailing issue. Concerning thermal comparison shown in [9], due to lower losses, SiC MOSFET had a 40°C lower operating case temperature (90.6°C temperature of SiC MOSFET and 131.5°C temperature of Si IGBT) which means that lighter and smaller heat sink can be used. Also, the SiC MOSFET converter at 100kHz requires (in a first order approximation) five times lighter inductor compared to that used for 20kHz Si IGBT converter, thus improving the power density.

Authors in [10] investigated and compared the performance of the Cree 1200V/100A SiC MOSFET module with the same rating Infineon silicon IGBT module. Experimental results in

[10] show that the Si IGBT compared to the SiC MOSFET at the same operating conditions (DC bus voltage  $V_{DC}=600V$ ; transistor current  $I_{ds}=100A$ ; gate resistance  $R_g=5\Omega$ ; junction temperature  $T_j=125^\circ C$ , and the SiC MOSFET operated at gate-source voltage  $V_{gs}=20V$ ) has a turn-on energy 3.6 times higher, a turn-off energy 6.8 times higher, and 11.2 times higher recovery energy.

However, some difficulties are encountered when using SiC components due to the high switching speed and frequency. One of the main issues is the high drain-source voltage ringing due to parasitic oscillation, especially the high frequency resonance between the parasitic capacitance of inductor and transistor and stray inductance in the switching power loop, which will lead to excessive ringing. Authors in [9] recommended using a single layer winding design for the inductor to reduce its parasitic capacitance and minimizing the switching loop for the PCB layout to minimize the stray inductance in these loops.

### A. SiC power module for 45kVA three-phase inverter

The CREE CAS100H12AM1 1200V - 100A SiC MOSFET Half-Bridge Module [11], shown in Fig. 1., is available on the market and can be a potential candidate for the MEA high power converter applications. The half bridge module has been packaged from discrete dies. Both the top and bottom devices are made from paralleling five 1200V, 80mΩ SiC MOSFETs and five 1200V, 10A SiC Schottky diodes [12]. The module has an equivalent on-state resistance  $R_{DSon}$  of 16mΩ at 25°C, thus low conduction losses. Using this module will boost the converter's efficiency and power density due to its low losses and compact lightweight packaging.

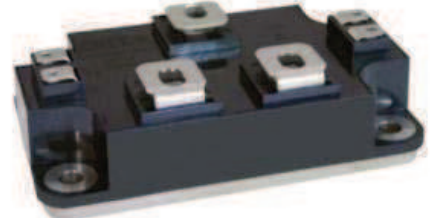


Fig. 1. 1200V/100A SiC MOSFET power module from manufacturer CREE. Reference CAS100H12AM1.

## III. SiC SWITCHING LOSSES MEASUREMENTS

### A. Switching Losses and Conventional Measurements

Unlike conduction losses, switching losses cannot always be obtained from values given in datasheets, due to the fact that they are sensibly dependent of the environment where switches are inserted, especially of parasitic inductances in different loops related to these components. Switching energy is a combination of stored, recovered and dissipated energy during the switching transitions, via several mechanisms:

- Transistor switching times (transition from off to on states and vice-versa, through the linear region).
- Body diode reverse-recovery energy.
- Energy stored in device capacitances and parasitic inductances.



The most common method to measure losses in a transistor is frequently called the “double pulse” method. However this method has serious drawbacks. The two most important of these drawbacks are:

- The shunt resistor or the current transformer used to measure the transistor’s current change the resistance and inductance of the commutation loop.
- The discharge current of the transistor’s parasitic capacitance is not measured by this method during turn-on. In the same manner, during turn-off, the current to charge the parasitic capacitance is measured by this method but the related energy is not lost during turn-off.

As a consequence, the calculated switching energy may be inaccurate, especially when it is applied to fast switches such as SiC or GaN transistor.

### B. Modified Opposition Method adapted for WBG Components

In the purpose of precisely measuring switching losses, a new method has been proposed to characterize the GaN and SiC transistors under real operating conditions [13]. The proposed method is a modified version of what authors in [14] call the “Opposition Method”. The opposition method, where the basic circuit is shown in Fig. 2, consists of an association of two identical converters supplied by the same source, one operating as a generator, the other as a receptor. An inductive link connects both converters and the control of the current flowing from one converter to the other is made by small differences applied to duty cycle of both converters. A modification of this method is made in order to estimate turn-on and turn-off losses separately. For that, measurements in two different modes must be done (Fig. 3). In the first mode, an AC current at the switching frequency is imposed through inductor  $L$ . Like this, transistors will only present turn-off losses, which can be estimated by using the measured losses of the converter. In the second mode, a DC current is imposed through inductor  $L$ . Thus, transistors will present turn-on and turn-off losses plus reverse recovery losses of diodes. Since turn-off losses were already estimated by the measurements in the first mode, one can then estimate losses at turn-on (turn-on losses of transistors plus reverse recovery losses of diodes) by using the measured losses of the second mode.

The power measured by this method is the total power dissipated by the system for a given operation point. In order to have an accurate estimation of switching losses, the other losses in the system must be estimated so they can be subtracted from the total measured power. These losses are:

#### 1) Inductor losses

They are divided into core and copper losses. Since a coreless inductor is sufficient for the setup due to high switching frequencies and high current amplitude in Mode 1, only copper losses are calculated. These losses are divided into DC and AC copper losses. DC copper losses are calculated using the DC resistance  $R_{DC}$  of the windings, while the AC copper losses are calculated using the inductor current harmonics and the winding AC resistance

corresponding to each harmonic. Thus total copper losses are calculated according to the following equation:

$$P_c = R_{DC} \cdot I_{DC}^2 + \sum_{m=1}^{\infty} R_{ACm} \cdot I_{m,rms}^2 \quad (1)$$

where  $R_{ACm}$  is the AC resistance at a given current harmonic calculated using analytical formulas or finite element simulations. An example of a simulated  $R_{AC}/R_{DC}$  ratio for a 9μH Litz wire inductor used in the experimental tests shown in Section IV, is given in Fig. 4.  $I_{DC}$  is the DC value of the inductor current and  $I_{m,rms}$  is the RMS value of the  $m^{th}$  harmonic of the high-frequency current flowing through the windings.

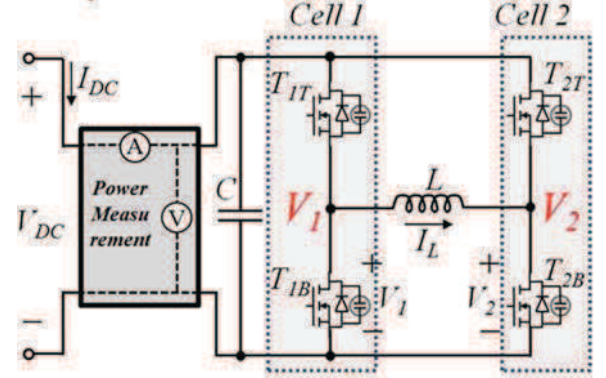


Fig. 2. Full bridge used in switching energy measurements of WBG components (opposition method).

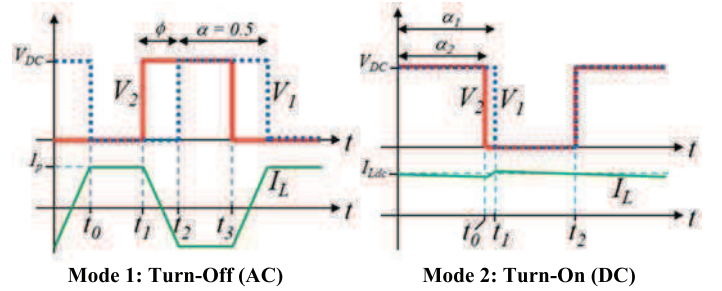


Fig. 3. Typical voltage and current waveforms used for the turn-off loss measurement mode and turn-on loss measurement mode.

#### 2) Transistor conduction losses

The on-state resistance  $R_{DSon}$  of the four transistors in the experimental setup have to be measured by regular static measurements at different junction temperatures and for a fixed gate-source voltage  $V_{gs}$ . Conduction losses can be then calculated using the measured  $R_{DSon}$  with the RMS value of the current flowing through them. Note that current is only measured at the inductor ( $I_L$ ) and with this measurement one can easily estimate transistor currents.

#### 3) Connection losses

They are mainly related to the copper loss on the PCB used for measurements and the connectors to the DC bus and the inductor. These losses are very low when compared to the other losses. Nevertheless they can be estimated by measuring the resistance of the PCB connections at different frequencies.

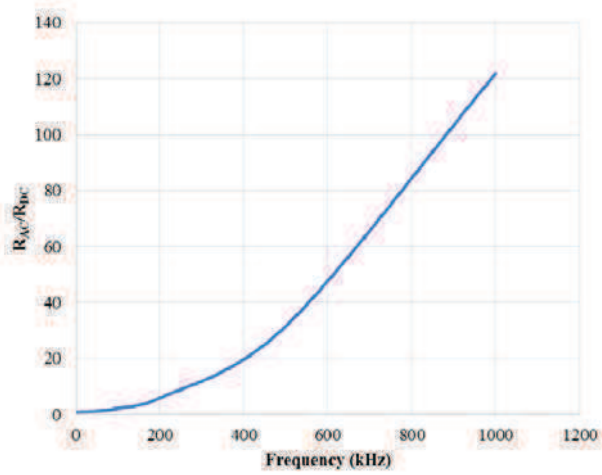


Fig. 4.  $R_{AC}/R_{DC}$  ratio for a 9  $\mu$ H Litz wire inductor used for calculating copper losses in equation (1).

#### 4) Bus capacitor losses

In DC mode, the current flowing through the capacitor is negligible and so are the capacitor losses. However, in the AC mode, high current can flow through the capacitors. Capacitor losses are then calculated with the current waveform and the capacitor's ESR given at the datasheet. They are usually negligible when compared to the other losses of the system.

Since both on-state resistance and inductor winding resistance vary with the temperature, temperatures rise in both SiC modules and inductor are measured and taken into account in the calculation of copper and conduction losses.

#### C. Test Bench and Module Test Board

A PCB with 70 $\mu$ m-thick copper layers was especially developed to test the CAS100H12AM1 SiC Module. The developed board is shown in Fig. 5. The combination of high voltage, high current and high switching speed of SiC MOSFETs requires careful consideration of the circuit layout to reduce the effects of parasitic capacitances and inductances. Two of these modules are used in the full bridge converter test board of the measurement setup, each forming a commutation cell. The drivers are connected as close as possible to the module in order to minimize the switching loop inductance for a cleaner switching waveform and more accurate loss measurements.

The experimental setup shown in Fig. 6 is composed of a DE2-115 FPGA board, which is controlled by a personal computer. The switching signals from the FPGA board are sent to an interface board, which converts the electrical signals in optical signals transmitted by fiber optics to the SiC test board. A high voltage source supplies the converter and total converter losses are measured by a DC voltmeter and ammeter. The test bench is enhanced by adding common mode filters to reduce EMI issues in the measurement instruments due to high speed switching.

## IV. EXPERIMENTAL RESULTS

Using the proposed method and the previously presented test

bench, switching energy of the CREE module is measured under real operating conditions. Different parameters altering the switching energy are varied, namely the, the DC bus Voltage  $V_{DC}$ , gate-source voltage  $V_{gs}$ , gate resistance  $R_g$  and dead time  $DT$ . The default values of these parameters are:  $V_{DC}=540$ V;  $V_{gs}=20$ V;  $R_g=1\Omega$  and  $DT=400$ ns. One parameter is varied at a time while keeping the other parameters at their default value. The resulting measured switching energies are shown in figures 7 to 10. In all these graphs, positive currents represent turn-off energy while negative currents represent turn-on energy.

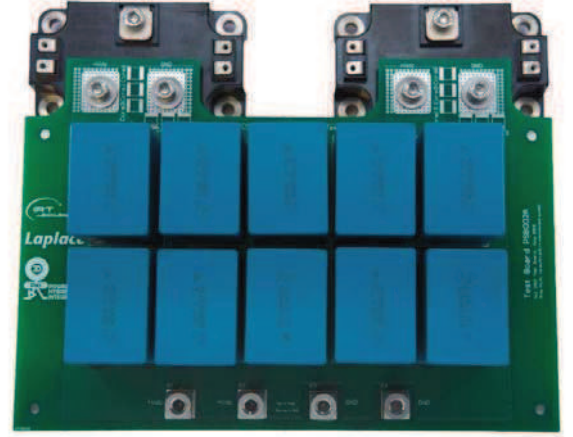


Fig. 5. Developed test board used for switching energy measurements specifically designed for the CAS100H12AM1 modules.

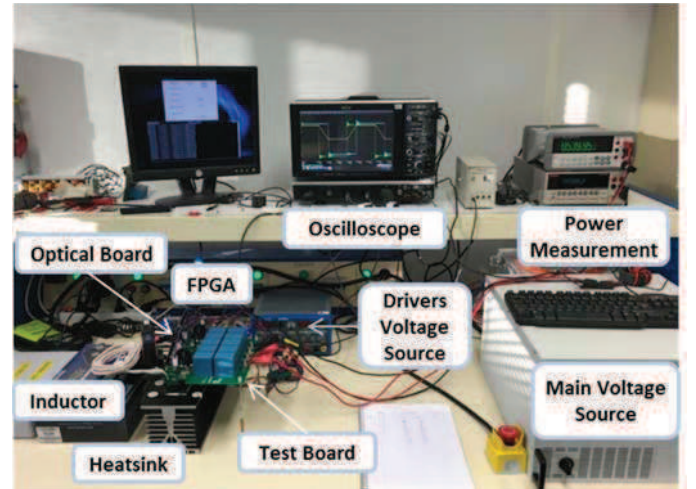


Fig. 6. Test bench used for switching energy measurements of WBG components.

Fig. 7 represents the switching energy as function of switching current ( $I_{sw}$ ) for different DC bus voltages (540V, 405V, 270V and 135V). As we can see that the switching energy increases with current and voltage as expected. The turn-off energy increases rapidly with current while the turn-on energy curves show a slight increase with current. Contrarily, the turn-on energy increases rapidly with voltage while the turn-off energy slightly increases with voltage. This can be explained mainly by the high parasitic inductances in the



commutation loop and the losses in the parasitic capacitance of the MOSFETs.

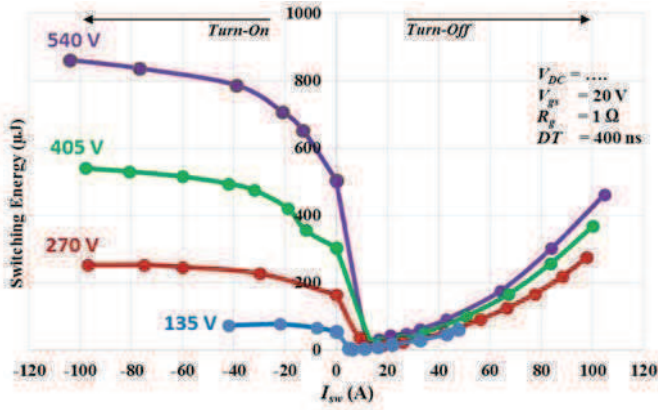


Fig. 7. Switching energy as function of switching current for different DC bus voltages ( $V_{DC}$ ).

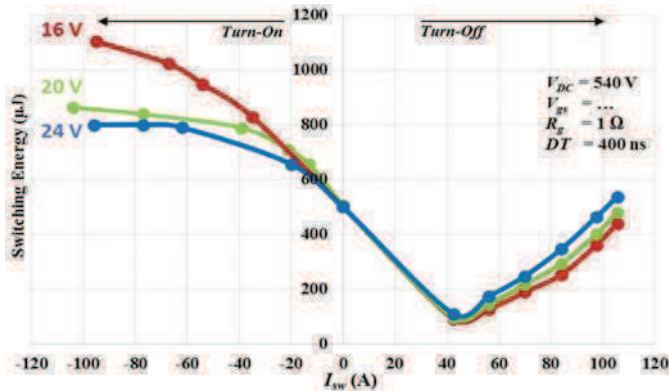


Fig. 8. Switching energy as function of switching current for different gate voltages ( $V_{gs}$ ).

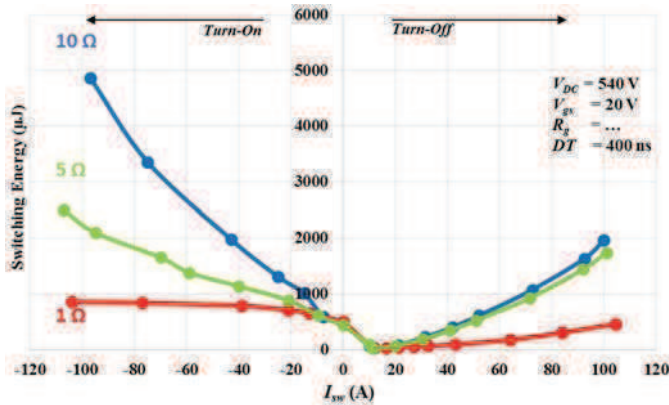


Fig. 9. Switching energy as function of switching current for different external gate resistances ( $R_g$ ).

Fig. 8 represents the switching energy as function of switching current as well, but for different  $V_{gs}$  (16V, 20V and 24V). Using higher  $V_{gs}$  would decrease total switching losses due to higher switching speed. Keeping in mind that the component's datasheet recommends a  $V_{gs}$  of 20V, using higher values (under the 25V component limit) may induce higher overvoltage and  $dv/dt$ .

Fig. 9 shows the switching energy as function of switching current for 3 different external gate resistances  $R_g$  (1Ω, 5Ω and 10Ω), knowing that this module has an internal gate resistance

of 1.25Ω. Clearly both turn-on and turn-off energies increase with the increase of gate resistance. The difference of switching energy can reach about five times between the highest and lowest switching energy (at 10Ω and 1Ω respectively). However, knowing that the minimum value used in the datasheet for the external gate resistance is 5Ω, using 1Ω instead would decrease switching losses to one third.

Fig. 10 shows the switching energy as function of switching current for different  $DT$  (80ns, 100ns, 200ns and 300ns). For low switching currents, losses increase with the increase of dead-time. This is due to the fact that at low currents the low dead-times are insufficient to charge and discharge the parasitic capacitor of the component. However, at high currents these capacitors are rapidly charged and discharged, thus even a small  $DT$  is sufficient, and the  $DT$  effect on losses is negligible.

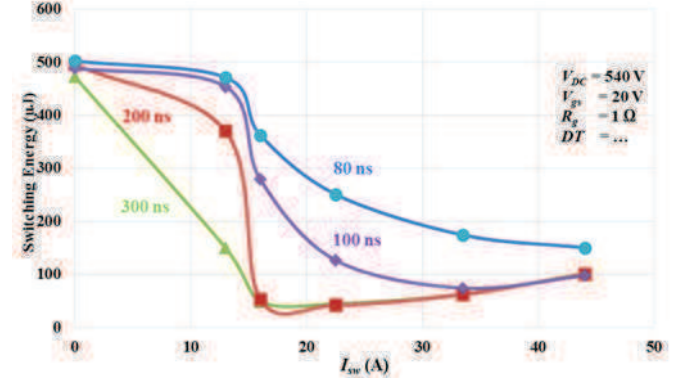


Fig. 10. Turn-off energy as function of switching current for different Dead Times ( $DT$ ).

Results shown in figures 7 to 10 allow us a better understanding of the CREE modules switching behavior and thus use them in the best way possible in the developed MEA converters.

To show the importance of the previous characterizations, the performance of the 1200V/100A SiC module is evaluated in a three phase 540V-45kVA inverter application. In fact the performance of the module is boosted compared to the datasheet based on the previous characterization results. An equivalent Si IGBT module is also considered in the comparison.

#### A. Expected gain using SiC MOSFET on MEAs

A MATLAB algorithm is developed to calculate transistors switching and conduction losses for different converter's switching frequencies and output current per phase. Four configurations are considered for the three-phase inverter design: 1 – using the Si IGBT SK100GB12T4 module (referred here as “IGBT Datasheet”); 2 – using the SiC module based on manufacturer's datasheet having  $R_g=5\Omega$  and  $V_{gs}=20V$  (referred here as “SiC datasheet R5”); 3 – using the same SiC module, however based on the previous characterizations having  $R_g=5\Omega$  and  $V_{gs}=20V$  (referred here as “SiC Measured R5”); 4 – using the same SiC module, based on the previous characterizations having  $R_g=1\Omega$  and  $V_{gs}=24V$  (referred here as “SiC Measured R1”). All SiC configurations have a 400ns

dead-time. The last configuration is the one where one can reduce the most losses in the SiC module. For the four different configurations, total losses are compared for RMS currents from 0 up to 80 A per phase and for two different switching frequencies  $F_{sw}$ , 15 kHz and 60 kHz. Calculation was made considering sinusoidal output currents in phase with the output voltage (i.e. resistive load), having negligible current ripple.

Fig. 11 shows transistors total losses of the three-phases of the inverter as function of current at 15 kHz and 60 kHz for the four configurations. At  $F_{sw}=60$  kHz and maximum current (80A), the "IGBT Datasheet" has about 1300W total losses, the two SiC configurations with  $R_g=5\Omega$  (based on the datasheet and measured data) has about 300W total losses while configuration SiC Measured R1" has about 160W total losses. That is, a factor of approximately 4 between "IGBT Datasheet" and "SiC Datasheet R5" losses while a factor of 8 between "IGBT Datasheet" and "SiC Datasheet R1" losses. Therefore, using the SiC module in the best way possible (concerning losses), will decrease total transistor losses by about 50% at  $F_{sw}=60$  kHz when compared to the configuration recommended by the manufacturer. The advantage of using the SiC the best way possible is obviously not so high at lower frequencies (note curves in Fig. 11 for  $F_{sw}=15$  kHz).

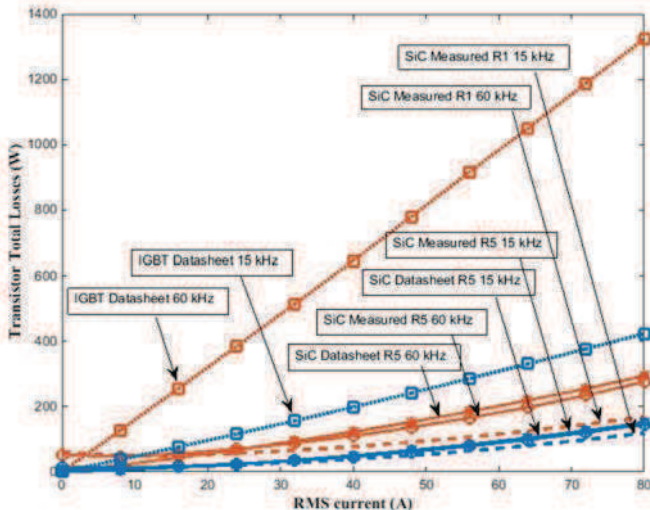


Fig. 11. Transistors total losses as function of current at 15 kHz and 60 kHz for the IGBT, SiC based on datasheet and SiC based on characterization ( $R$  indicates the external gate resistance value, in ohms).

## V. CONCLUSION

In the aim of replacing the Si by SiC semiconductors in near-future on more electrical aircrafts, this paper investigates the behavior of the promising candidates SiC modules under different operating conditions. Their enhanced behavior based on varying switching parameters ( $R_g$ ,  $V_{gs}$ ,  $DT$  and others) is compared to conventional behavior based on datasheet values. An equivalent Si IGBT module is also considered in the comparison to show the advantages of SiC over Si components. A method adapted for characterizing SiC transistors has been explained along with the test bench and developed test boards. Experimental results show the variation

of switching energy with switching current and different switching parameters. Based on the experimental results, the design of a three phase 540V-45kVA inverter using the SiC module in the enhanced mode is investigated to show an improvement of 50% on total losses compared to a conventional usage of SiC module based on datasheet values.

Nevertheless, the improvements on switching losses are compromised by high switching speeds and voltage overshoot, which are two important aspects in the aeronautics domain. Both should be taken into account to minimize their effect on Electromagnetic Interference and Partial Discharge which can occur in the cables and motors connected to the converter using SiC modules. These aspects are points of interest for a future work.

## REFERENCES

- [1] B. Sarioglu, C.T. Morris, "More Electric Aircraft: Review, Challenges, and Opportunities for Commercial Transport Aircraft," in *Transportation Electrification, IEEE Transactions on*, vol.1, no.1, pp.54-64, June 2015
- [2] R.T. Naayagi, "A review of more electric aircraft technology," in *Energy Efficient Technologies for Sustainability (ICEETS), 2013 International Conference on*, vol., no., pp.750-753, 10-12 April 2013
- [3] K.C. Reinhardt, M.A. Marciniak, "Wide-bandgap power electronics for the More Electric Aircraft," in *Energy Conversion Engineering Conference, 1996. IECEC 96., Proceedings of the 31st Intersociety*, vol.1, no., pp.127-132 vol.1, 11-16 Aug 1996
- [4] J. Biela, M. Schweizer, S. Waffler, J. W. Kolar, "SiC versus Si - Evaluation of Potentials for Performance Improvement of Inverter and DC-DC Converter Systems by SiC Power Semiconductors," *IEEE Transactions on Industrial Electronics*, Vol. 58, No. 7, pp. 2872-2882, July 2011
- [5] J. Biela, M. Schweizer, S. Waffler, J. W. Kolar, "SiC versus Si - Evaluation of Potentials for Performance Improvement of Inverter and DC-DC Converter Systems by SiC Power Semiconductors," *IEEE Transactions on Industrial Electronics*, Vol. 58, No. 7, pp. 2872-2882, July 2011.
- [6] R. Wang, D. Boroyevich, P. Ning, Z. Wang, F. Wang, P. Mattavelli, K. Ngo, and K. Rajashekara, "A high-temperature SiC three-phase ac-dc converter design for  $> 100^\circ\text{C}$  ambient temperature," *IEEE Transactions on Power Electronics*, vol. 28, no. 1, pp. 555-572, Jan. 2013.
- [7] L. Prisse, D. Ferer, H. Foch, A. Lacoste, "New power centre and power electronics sharing in aircraft", 13th European Conference on Power Electronics and Applications (EPE), Barcelona, Spain. Sept. 2009.
- [8] X. Giraud, M. Budinger, X. Roboam, H. Piquet, M. Sartor, J. Faucher, "Optimal desing of the integrated modular power electronics cabinet", *Aerospace Science and Technology*, vol. 48, pp. 37-52, 2016.
- [9] J. Liu and K. L. Wong, "Performance Evaluation of Hard-Switching Interleaved DC/DC Boost Converter with New Generation Silicon Carbide MOSFETs," CREE, Durham, NC, USA.
- [10] Wang Gangyao, Wang Fei, G Magai, Lei Yang, A. Huang, M. Das, "Performance comparison of 1200V 100A SiC MOSFET and 1200V 100A silicon IGBT," *IEEE Energy Conversion Congress and Exposition (ECCE)*, pp.3230-3234, 15-19 Sept. 2013;
- [11] CREE CAS100H12AM1 1200V 100A SiC MOSFET module datasheet: <http://www.cree.com/power/products/sic-powermodules/sic-modules/cas100h12am1>.
- [12] M. K. Das, "SiC MOSFET Module Replaces up to 3x Higher Current Si IGBT Modules in Voltage Source Inverter Application," *Bodo's Power Systems*, pp. 22-24, Feb. 2013.
- [13] B. Cougo, H. Schneider, T. Meynard, "Accurate switching energy estimation of wide bandgap devices used in converters for aircraft applications," 15th European Conference on Power Electronics and Applications (EPE), Lille, France. 2-6 Sept. 2013.
- [14] F. Forest, J.-J. Huselstein, S. Faucher, M. Elghazouani, P. Ladoux, T. A. Meynard, F. Richardeau, C. Turpin, "Use of opposition method in the test of high-power electronic converters", *IEEE Transactions on Industrial Electronics*, vol.53, no.2, pp. 530- 541, April 2006